Finite element analysis of Volterra dislocations in anisotropic crystals: A thermal analogue

A. E. Giannakopoulos*[§], K. P. Baxevanakis*, A. Gouldstone**

*Laboratory of Strength of Materials and Micromechanics, University of Thessaly, Volos, 38334, Greece
**Stony Brook University, Stony Brook, NY 11794-2275, USA

Abstract

The present work gives a systematic and rigorous implementation of Volterra dislocations in ordinary two-dimensional finite elements using the thermal analogue and the integral representation of dislocations through the stresses. The full fields are given for edge dislocations in anisotropic crystals and the Peach-Koehler forces are found for some important examples.

Keywords: Dislocations, Finite Elements, Anisotropic Elasticity.

1. Introduction

Dislocations are line defects in crystalline materials with well documented existence, formation, interaction and motion. Their importance in science and technology is enormous. The mechanics of dislocations is a prominent and difficult subject of Linear Elasticity, Hirth and Lothe (1982). Closed form solutions exist for relatively simple problems, whereas more complex geometries, as well as anisotropy, introduce substantial difficulties. In many cases, the detailed stress fields around dislocations are not known explicitely, especially when dislocations are interacting with boundaries or other dislocations.

The knowledge of the stresses around dislocations is important. The equilibrium position of a dislocation and its stability requires that the resulting shear stress be balanced by the non-linear atomic interactions across the glide plane. This resisting to the free motion stress is called the Peierls stress, Peierls (1940) and Nabarro (1947). The assessment of such stresses is important for the physical theories of plasticity, fatigue and fracture, micro and nano-indentation, strength of nano-composites and micro-electro-mechanical devices etc (see for example Phillips, 2001; Cotrell, 1961; Petch, 1953; Hall, 1951; Rice, 1992).

Atomistic calculations are still not in regular engineering use, despite important attempts to be included in finite element methodologies, e.g. Tadmor et al. (1996). In the present work we use an analogue from thermoelasticity to describe discrete dislocations within the context of classic finite element methodology. Biot (1935) presented a thermal analogue to model the elastic fields around dislocations and the method has been applied as an experimental technique to study dislocations with optical methods. The integral representation of the Burgers vector in terms of stresses has been shown by Mindlin and Salvadori (1950) and has been recently used by Dundurs and Markenscoff (1993). We use the previous ideas, together with a suitable

[§] Associate Professor, Head of the Laboratory of Strength of Materials and Micromechanics
Tel.: +24210-74179, Fax:+24210-74169, E-mail: agiannak@uth.gr

temperature distribution to circumvent the displacement incompatibility that is needed by the mathematical description of a Volterra dislocation, however, not allowed by ordinary finite elements. The present work is focusing on the two-dimensional edge dislocations in anisotropic crystals, following our initial work on isotropic materials, Gouldstone and Giannakopoulos (2005).

2. The thermal analogue and its implementation in finite elements

2.1. The thermal analogue for two dimensional edge dislocations

We will consider an elastic solid under plane deformation. In the absence of body forces, the contents of the stress tensor σ_{ij} must obey the equilibrium conditions which in Cartesian coordinates (x, y, z) are:

$$\frac{\partial \sigma_{xx}}{\partial x} + \frac{\partial \sigma_{yx}}{\partial y} = 0 \quad \text{and} \quad \frac{\partial \sigma_{xy}}{\partial x} + \frac{\partial \sigma_{yy}}{\partial y} = 0 \tag{1}$$

The linear strain components must meet the local compatibility condition

$$\frac{\partial^2 \varepsilon_{yy}}{\partial x^2} - 2\frac{\partial^2 \varepsilon_{xy}}{\partial x \partial y} + \frac{\partial^2 \varepsilon_{xx}}{\partial y^2} = 0 \tag{2}$$

Consider an Airy function $\Phi(x, y)$ so as (1) are satisfied

$$\sigma_{xx} = \frac{\partial^2 \Phi}{\partial y^2} \quad , \quad \sigma_{yy} = \frac{\partial^2 \Phi}{\partial x^2} \quad , \quad \sigma_{xy} = -\frac{\partial^2 \Phi}{\partial x \partial y} \tag{3}$$

The local compatibility condition is necessary for given strain components to yield continuum displacements (u_x, u_y), but is not sufficient if the domain is multiply connected. According to Michell (1899), global compatibility conditions in the form of line integrals must be imported. For closed contours surrounding a Volterra dislocation (Fig. 1):

$$\oint d\omega_z = 0 \text{ where } \omega_z = \frac{1}{2}\left(\frac{\partial u_y}{\partial x} - \frac{\partial u_x}{\partial y}\right) \text{ is the material rotation} \tag{4}$$

$$\oint du_x = b_x \text{ and } \oint du_y = b_y \tag{5}$$

Equation (4) is necessary in order not to have any edge disclination (Somigliana type of dislocation). The quantities b_x and b_y are the components of the Burgers vector of an edge dislocation.

[Figure 1]

Recall the strain-displacement relations

$$\varepsilon_{xx} = \frac{\partial u_x}{\partial x}, \ \varepsilon_{yy} = \frac{\partial u_y}{\partial y}, \ \varepsilon_{xy} = \frac{1}{2}\left(\frac{\partial u_x}{\partial y} + \frac{\partial u_y}{\partial x}\right) \tag{6}$$

Then equation (4) becomes:

$$0 = \oint\left[\left(\frac{\partial \varepsilon_{xy}}{\partial x} - \frac{\partial \varepsilon_{xx}}{\partial y}\right)dx + \left(\frac{\partial \varepsilon_{yy}}{\partial x} - \frac{\partial \varepsilon_{xy}}{\partial y}\right)dy\right] \tag{7}$$

Taking into account equations (5), (6), (7) and (2), we obtain:

$$b_x = -\oint x\left(\frac{\partial \varepsilon_{xx}}{\partial x}dx - \frac{\partial \varepsilon_{xx}}{\partial y}dy\right) - \oint y\left[\frac{\partial \varepsilon_{xx}}{\partial x}dx - \left(\frac{\partial \varepsilon_{yy}}{\partial y} - 2\frac{\partial \varepsilon_{xy}}{\partial y}\right)dy\right] \tag{8}$$

$$b_y = -\oint x\left[\left(2\frac{\partial \varepsilon_{xy}}{\partial x} - \frac{\partial \varepsilon_{xx}}{\partial y}\right)dx + \frac{\partial \varepsilon_{yy}}{\partial x}dy\right] - \oint y\left(\frac{\partial \varepsilon_{yy}}{\partial x}dx + \frac{\partial \varepsilon_{yy}}{\partial y}dy\right) \tag{9}$$

Let us consider the tangent and the perpendicular vectors of the closed contours (Fig. 1):

$$\underset{\sim}{\mathbf{n}} = \left\{ \frac{dy}{ds}, -\frac{dx}{ds} \right\}^T , \qquad \underset{\sim}{\mathbf{s}} = \left\{ \frac{dx}{ds}, \frac{dy}{ds} \right\}^T \tag{10}$$

$$\frac{\partial}{\partial n} ds = \frac{\partial}{\partial x} dy - \frac{\partial}{\partial y} dx , \qquad \frac{\partial}{\partial s} ds = \frac{\partial}{\partial x} dx + \frac{\partial}{\partial y} dy \tag{11}$$

Next, consider an anisotropic thermoelastic medium with cubic crystal symmetry in its elastic properties (3 elastic constants are needed: c_{11}, c_{12}, c_{44}). The constitutive expressions between the strains and the stresses in plane-strain deformation are:

$$\varepsilon_{xx} = \frac{1+\nu}{E}\left[\sigma_{xx} - \nu\left(\sigma_{xx} + \sigma_{yy}\right)\right] + \alpha(1+\nu)\theta \tag{12}$$

$$\varepsilon_{yy} = \frac{1+\nu}{E}\left[\sigma_{yy} - \nu\left(\sigma_{xx} + \sigma_{yy}\right)\right] + \alpha(1+\nu)\theta , \qquad \varepsilon_{xy} = \frac{1}{2\mu}\sigma_{xy}$$

In the absence of the temperature distribution θ(x, y), the stresses relate to the deformations in the following way:

$$\left\{\sigma_{ij}\right\} = \left\{c_{ijkl}\right\}_{6\times 6}\left\{\varepsilon_{kl}\right\} \tag{13}$$

Taking into account the equations above, we obtain

$$\mu = c_{44} , \qquad \nu = \frac{c_{12}}{c_{11} + 2c_{12}} , \qquad E = \frac{\left(c_{11} - c_{12}\right)\left(c_{11} + 3c_{12}\right)}{c_{11} + 2c_{12}} \tag{14}$$

$H = 2c_{44} + c_{12} - c_{11}$ is the anisotropy factor and $A = \dfrac{2c_{44}}{c_{11} - c_{12}}$ is the anisotropy ratio (see Table 1 for particular examples used in this work).

From the Michell equations (8) and (9) and from continuity of $x\sigma_{xx}$, $y\sigma_{xy}$ and $y\sigma_{xx}$, $x\sigma_{xy}$ we obtain:

$$\begin{aligned} b_x = {} & \alpha(1+\nu)\oint\left(x\frac{\partial\theta}{\partial s} - y\frac{\partial\theta}{\partial n}\right)ds + \frac{\left(1-\nu^2\right)}{E}\oint\left(x\frac{\partial\left(\sigma_{xx}+\sigma_{yy}\right)}{\partial s} - y\frac{\partial\left(\sigma_{xx}+\sigma_{yy}\right)}{\partial n}\right)ds \\ & -\frac{(1+\nu)}{E}\oint\left(\sigma_{xy}n_x + \sigma_{yy}n_y\right)ds + \left(\frac{1}{\mu} - \frac{2(1+\nu)}{E}\right)\oint\sigma_{xy}dy \end{aligned} \tag{15}$$

$$\begin{aligned} b_y = {} & \alpha(1+\nu)\oint\left(x\frac{\partial\theta}{\partial n} + y\frac{\partial\theta}{\partial s}\right)ds + \frac{\left(1-\nu^2\right)}{E}\oint\left(x\frac{\partial\left(\sigma_{xx}+\sigma_{yy}\right)}{\partial n} + y\frac{\partial\left(\sigma_{xx}+\sigma_{yy}\right)}{\partial s}\right)ds \\ & +\frac{(1+\nu)}{E}\oint\left(\sigma_{xx}n_x + \sigma_{xy}n_y\right)ds + \left(\frac{2(1+\nu)}{E} - \frac{1}{\mu}\right)\oint\sigma_{xy}dx \end{aligned} \tag{16}$$

From the compatibility equation, we obtain

$$\frac{\left(1-\nu^2\right)}{E}\left[\frac{\partial^4\Phi}{\partial x^4} + \frac{\partial^4\Phi}{\partial y^4} + 2\frac{\partial^4\Phi}{\partial x^2\partial y^2}\right] + \left(\frac{1}{\mu} - \frac{2(1+\nu)}{E}\right)\frac{\partial^4\Phi}{\partial x^2\partial y^2} = -\alpha\left(1+\nu\right)\left(\frac{\partial^2\theta}{\partial x^2} + \frac{\partial^2\theta}{\partial y^2}\right) \tag{17}$$

Also recall that all stresses are continuous so that

$$\oint\sigma_{xy}dy = 0 , \ \oint\sigma_{xy}dx = 0 , \ \nabla^2\Phi = -\frac{\alpha(1+\nu)\theta}{\dfrac{\left(1-\nu^2\right)}{E} + \dfrac{1}{2}\left(\dfrac{1}{\mu} - \dfrac{2(1+\nu)}{E}\right)} = \sigma_{xx} + \sigma_{yy} \tag{18}$$

From overall equilibrium of the tractions at the contours we have:

$$\oint\left(\sigma_{xy}n_x+\sigma_{yy}n_y\right)ds=0 \quad , \quad \oint\left(\sigma_{xx}n_x+\sigma_{xy}n_y\right)ds=0 \tag{19}$$

Now assume a steady state thermal distribution:

$$\left(\frac{\partial^2}{\partial x^2}+\frac{\partial^2}{\partial y^2}\right)\theta=0 \tag{20}$$

Then, eqs. (2) and (7) hold true and eqs. (15) and (16) become:

$$b_x=-(1+\nu)a\oint\left(y\frac{\partial\theta}{\partial n}-x\frac{\partial\theta}{\partial s}\right)ds \quad , \quad b_y=(1+\nu)a\oint\left(y\frac{\partial\theta}{\partial s}+x\frac{\partial\theta}{\partial n}\right)ds \tag{21}$$

The temperature θ must satisfy equation (20) in order to avoid disclinations. As an example, select θ(x, y) as:

$\theta=\Delta T$	y=0	x≤0
$\theta=\Delta T\dfrac{y+h}{h}$	h≤y≤0	x≤0
$\theta=\Delta T\dfrac{h-y}{h}$	0≤y≤h	x≤0
$\theta=0$ everywhere else		

(22)

The distribution described by (22) satisfies (20) and when inserted in (21) gives

$$b_y=-2(1+\nu)\alpha\Delta Th \tag{23a}$$

In a similar way (by selecting an appropriate temperature distribution), we can obtain

$$b_x=2(1+\nu)\alpha\Delta Th \tag{23b}$$

Note that eqs. (21) are the key theoretical results that need to be implemented in the finite element codes and then, after selecting an appropriate temperature field as in (22), solve the resulting thermoelastic problem.

[Figure 2]

2.2. Finite elements implementation

Turning to the Finite Element Method, assume that around the edge dislocation there is a fine element distribution of element size h, Fig. 2. Assuming linear thermoelastic response, we can assign a temperature distribution as in equations (22), on the dashed strips of elements shown in Fig. 2, with

$$\Delta T=-\frac{b_y}{2(1+\nu)\alpha_y h}, \qquad a_y=a, \qquad a_x=0, \qquad a_z=0 \tag{24}$$

and/or

$$\Delta T=\frac{b_x}{2(1+\nu)\alpha_x h}, \qquad a_x=a, \qquad a_y=0, \qquad a_z=0 \tag{25}$$

so that effectively an edge dislocation with predefined components of the Burgers vector (b_x, b_y) is inserted through a temperature distribution. It should be noted that the thermal expansion coefficients α_x, α_y (α_z = 0 in all cases) are not the physical ones, but take apparent values that are suitable for the computations, keeping in mind that there is no actual temperature field in the problem. This procedure forces ordinary finite elements to produce dislocation stress fields in a straightforward way. It should also be reminded that the finite element enforcement of the integrals (21) is done through Gauss integration at selected points and therefore, the type of element is important for the precise implementation of (21). If four-noded elements are to be used, then the inputs (24) and (25) need to be multiplied by 1/0.57735.

The ABAQUS general purpose finite element code was used and a mesh of 10000 four-noded elements was picked for all applications. The outer boundary was 150 times the Burgers vector in all directions, to model the conditions at infinity, $\sigma_{ij} \to O\left(\frac{1}{\sqrt{x^2+y^2}}\right)$ as $\sqrt{x^2+y^2} \to \infty$. Note that no special attention was taken for mesh optimization (which will be presented in future work).

[Figure 3]

3. Numerical examples

3.1. Single edge dislocations

An edge dislocation under plane strain, in an isotropic infinite medium, produces the following classic stresses:

$$\sigma_{xx} = -\frac{\mu b}{2\pi(1-\nu)}\frac{y(3x^2+y^2)}{\left(x^2+y^2\right)^2}, \qquad \sigma_{yy} = -\frac{\mu b}{2\pi(1-\nu)}\frac{y(x^2-y^2)}{\left(x^2+y^2\right)^2}, \tag{26}$$

$$\sigma_{xy} = \frac{\mu b}{2\pi(1-\nu)}\frac{x(x^2-y^2)}{\left(x^2+y^2\right)^2}, \quad \sigma_{zz} = \nu(\sigma_{xx}+\sigma_{yy}) = -\frac{\mu b\nu}{\pi(1-\nu)}\frac{y}{x^2+y^2}, \quad \sigma_{xz} = \sigma_{yz} = 0$$

[Table 1]

The corresponding stresses around an edge dislocation in anisotropic infinite medium have been found by Eshelby et al. (1955) and are:

$$\sigma_{xx} = \frac{Mb_x}{2\pi\rho^4 c'_{22}}\left\{\left[\left(\bar{c}'_{11}-c'_{12}\right)\left(\bar{c}'_{11}+c'_{12}+2c'_{66}\right)-\bar{c}'_{11}c'_{66}\right]x^2y+\frac{\bar{c}'^2_{11}c'_{66}}{c'_{22}}y^3\right\}+\frac{Mb_y c'_{66}}{2\pi\rho^4}\left(\frac{\bar{c}'_{11}}{c'_{22}}xy^2-x^3\right)$$

$$\sigma_{yy} = \frac{Mb_x c'_{66}}{2\pi\rho^4}\left(-x^2y+\frac{\bar{c}'_{11}}{c'_{22}}y^3\right)-\frac{Mb_y}{2\pi\rho^4\bar{c}'_{11}}\left\{\left[\left(\bar{c}'_{11}-c'_{12}\right)\left(\bar{c}'_{11}+c'_{12}+2c'_{66}\right)-\bar{c}'_{11}c'_{66}\right]xy^2+c'_{22}c'_{66}x^3\right\}$$

$$\sigma_{xy} = \frac{Mb_x c'_{66}}{2\pi\rho^4}\left(-x^3+\frac{\bar{c}'_{11}}{c'_{22}}xy^2\right)+\frac{Mb_y c'_{66}}{2\pi\rho^4}\left(-x^2y+\frac{\bar{c}'_{11}}{c'_{22}}y^3\right) \tag{27}$$

where $M = \left(\bar{c}'_{11}+c'_{12}\right)\left[\frac{\bar{c}'_{11}-c'_{12}}{c'_{22}c'_{66}\left(\bar{c}'_{11}+c'_{12}+2c'_{66}\right)}\right]^{1/2}$

$$\rho^4 = \left(x^2+\frac{\bar{c}'_{11}}{c'_{22}}y^2\right)^2+\frac{\left(\bar{c}'_{11}+c'_{12}\right)\left(\bar{c}'_{11}-c'_{12}-2c'_{66}\right)}{c'_{22}c'_{66}}x^2y^2 \tag{28}$$

$$\bar{c}'_{11} = \left(c'_{11}c'_{22}\right)^{1/2}, \quad c'_{11} = c_{11}, \quad c'_{12} = c_{12}, \quad c'_{66} = c'_{55} = c_{44}, \quad c'_{22} = c_{11}+\frac{1}{2}H$$

With these expressions we obtain the stresses fields shown in the following figures 4 and 5. For brevity, we show only the σxx fields which are the ones that are influenced mostly by the anisotropy. The left parts of the Figures are the finite element predictions whereas the right parts are the theoretical predictions.

[Figures 4a,

4b, 5a, 5b]

3.2. Influence of a free surface

Consider an edge dislocation with **b** = (0, b_y), at a distance *l* from a free surface, Fig. 6.

[Figure 6]

The stress fields in this occasion are not symmetric as in the dislocation in an infinite medium and can be found in the book of Hirth and Lothe (1982). Such asymmetry will create a configurational (material) force on the dislocation, no other that the Peach-Koehler force (Peach and Koehler, 1950). The Peach-Koehler force per unit dislocation length that will attempt to move the dislocation is given by the form

$$F_k = -\varepsilon_{ijk}\xi_i\sigma_{jl}b_l \quad \text{or} \quad \mathbf{F} = \mathbf{G}\times\boldsymbol{\xi} = \left(G_y\xi_z\right)\mathbf{i} + \left(-G_x\xi_z\right)\mathbf{j} \tag{29}$$

where $\xi_z = 1$ is the direction of the dislocation line (in this case in the out-of-plane direction z) and

$$G_x = \sigma_{xx}b_x + \sigma_{xy}b_y \quad , \quad G_y = \sigma_{yx}b_x + \sigma_{yy}b_y \tag{30}$$

The resulting force is an attraction toward the free surface and is equal to

$$F_y = \frac{\mu b_y^2}{4\pi(1-\nu)l} = -\frac{\Delta W}{\Delta s} = -\frac{W'-W}{\Delta s}, \qquad F_x = 0 \tag{31}$$

Consider that the dislocation's distance from the free surface is l=13b_y and the material is W. From eq. (31) and table 1, we obtain the theoretical solution of the acting force, $F_y = \frac{\mu b_y^2}{4\pi(1-\nu)l} = \frac{16 b_y^2}{4\pi(1-0.218)13 b_y} = 0.125$ b_y $\times10^{10}$ (N/m).
Calculating the force in terms of stresses, we lead in F_y=0.170 b_y $\times10^{10}$ (N/m). We can improve the precision of that result by doing a cubic interpolation near the tip and reach to F_y=0.167 $b_y \times10^{10}$ (N/m), that is an overestimation of 34%.
It is clear that the poor resolution of the mess (13 elements between the dislocation and the free surface) seems to be inadequate for an exact evaluation of (F_x, F_y) although the overall stress distribution seem to be accurate.
To improve the estimation of (F_x, F_y), without changing the mesh density, an alternative methodology is proposed, based on the energy released by a small advancement of the dislocation in the x and y directions respectively. Then,

$$F_x = -\frac{\partial U}{\partial x}, \qquad F_y = -\frac{\partial U}{\partial y} \tag{32}$$

where U is the total elastic energy of the material with the dislocation. In the numerical implementation of eq. (32), we move the dislocation (and the associate temperature distribution) by one finite element of length h in the (positive) x and the (positive) y direction, separately. Then, we compute the total energy in the initial and in the new positions of the dislocation to find the changes of energy ΔU. The forces were computed from the discretized form of eq. (32) with Δx=h and Δy=h respectively.

$$F_x = -\frac{\Delta U}{\Delta x} = -\frac{U_{new} - U_{initial}}{h}, \qquad F_y = -\frac{\Delta U}{\Delta y} = -\frac{U_{new} - U_{initial}}{h} \tag{33}$$

In terms of the change of the total energy of the system, we obtain an almost exact result $F_y = 0.1056\frac{\mu b_y^2}{l}$ (N/m) and F_x=0. In the same way, for Cu, we obtain

$F_y = 0.0802\frac{\mu b_y^2}{l}$ (N/m), F_x=0 and $F_y = 0.0698\frac{\mu b_y^2}{l}$ (N/m), F_y=0 if the crystal is rotated by 90°. Whether the dislocation will actually move towards the free surface will depend on the opposing Peierls force (Peierls, 1940; Nabarro, 1947) $\tau_p \cdot L$ where L is the length of the dislocation. For Cu, the value of the Peierls stress is given in the following table (b=0.255 nm, τ_p=2.43 MPa).

For a dislocation length L=1m, the minimum distance to avoid attraction of the dislocation towards the free surface for the two cases of Cu crystal is *l*=1.619 μm and *l*=1.409 μm respectively. The isotropic approximation gives $F_y = 0.1129\frac{\mu b_y^2}{l}$ (N/m) and *l*=2.279μm.

[Table 2]
[Figure 7]

4. Conclusions and further work

The present work gives the development of a robust finite element computational tool for two dimensional edge dislocations in anisotropic crystals. Existing analytical solutions were checked and completed with presentations of the full stress fields. Extensive presentations of dislocation interactions with material interfaces, grain boundaries, spherical particles etc. will be given in future work. The method can be extended to study dynamic dislocations, dislocations in piezoelectrics, the influence of large deformations and disclinated dislocations (to model better the dislocation cores).

Acknowledgements
The authors are grateful to Prof. N. Aravas for allowing the use of the computational facilities of the Laboratory for Computational Mechanics.

References

[1] ABAQUS Version 6.4 Finite Element Code. Hibbitt, Karlsson and Sorensen, Inc., Pawtucket, R. I.
[2] Barnett DM (1999) Elastic Anisotropy, Mechanics and Materials: Fundamentals and Linkages. Edited by M. A. Heyers, R. W. Armstrong, H. Kirchner. John Wiley & Sons, pp 71-98
[3] Biot MA (1935) Distributed gravity and temperature loading in two dimensional elasticity replaced by boundary pressures and dislocations. J. Appl. Mech. IV(2):A41-45
[4] Cotrell AH (1961) *Dislocations and Plastic Flow in Crystals*. Oxford University Press, London
[5] Dundurs J, Markenscoff X (1993) Invariance of stresses under a change in elastic compliances. Proc. R. Soc. London A, A443:289-300
[6] Eshelby JD, Read WT, Shockley W (1953) Anisotropic Elasticity with applications to dislocation theory. Acta Metallurgica 1:251-259
[7] Gouldstone A, Giannakopoulos AE (2005) A finite element method for plain-strain and axisymmetric problems of microstructures with dislocations, under preparation

[8] Hall EO (1951) The deformation and ageing of mid steel: III discussion of results. Proc. Phys. Soc. London, Sect B, 64:747-53
[9] Hirth JP, Lothe J (1982) *Theory of Dislocations*, 2nd edition. John Wiley & Sons, New York
[10] Michell JH (1899) On the direct determination of stress in an elastic solid, with application to the theory of plates. Proc. London Math. Soc.31:100-124
[11] Mindlin RD, Salvadori MG (1950) In Handbook of experimental stress analysis. Edited by M. Hetenyi. John Wiley & Sons, New York, pp 700-827
[12] Nabarro FRN (1947) Dislocations in a single cubic lattice. Proc. Phys. Soc. 59:256-272
[13] Nabarro FRN (1997) Theoretical and experimental estimates of the Peierls stress. Phil. Mag. A75:703-711
[14] Peach M, Koehler JS (1950) The forces exerted on dislocations and the stress fields produced by them. Physical Review 80:436-439
[15] Peierls R (1940) The size of a dislocation. Proc. Phys. Soc.52:34-37
[16] Petch NJ (1953) The cleavage strength of polycrystals. J. Iron Steel. Inst. 174:25-8
[17] Phillips R (2001) *Crystals, Defects and Microstructures: Models Across Scales*. Cambridge University Press.
[18] Rice JR (1992) Dislocation nucleation from a crack tip: An analysis based on the Peierls concept. J. Mech. Phys. Solids 40:239-271
[19] Tadmor EB, Ortiz M, Phillips R (1996) Quasicontinuum analysis of defects in solids. Phil. Mag. A73:1529-1563
[20] Wang JN (1996) Prediction of Peierls stresses for different crystals. Mater. Sci. Eng. A206:259-269

Table 1: Elastic constants of Cr, Cu and W (after Hirth and Lothe, 1982).

Crystal	c_{11} (10^{10} Pa)	c_{12} (10^{10} Pa)	c_{44} (10^{10} Pa)	H (10^{10} Pa)	A	μ (10^{10} Pa)	E (10^{10} Pa)	v
Cr	35.00	5.78	10.10	-9.02	0.69	10.10	32.85	0.124
Cu	16.84	12.14	7.54	10.38	3.21	7.54	6.09	0.295
W	52.10	20.10	16.00	0.00	1.00	16.00	38.97	0.218

Table 2: Predominant slip systems and corresponding Peierls stresses for Cu (after Wang, 1996).

Material	Structure	Burgers vector and length b	Primary slip system d {plane}/b <direction>	Theoretical τ_p/μ at 0° K	Experimental τ_p/μ at 0° K
Cu	Simple fcc	$\langle 1\bar{1}0\rangle, a_0\sqrt{2}/2$ b=0.255 nm	$\frac{\sqrt{6}}{3}a_0\{111\} \Big/ \frac{\sqrt{2}}{2}a_0\langle 1\bar{1}0\rangle$	3.22×10^{-5}	5.31×10^{-6} 1.04×10^{-5}

Figure 1: The components of the Burgers vector of an edge type Volterra dislocation and the corresponding contours surrounding them.
Figure 2: The implementation of the thermal analogue to finite elements.

Figure 3: The normalized stresses σ_{xx}/b_y for material W. The Burgers vector is **b**=(0, b_y). The isocontours range is (2.0, -2.0) Pa/m. On the left are the finite element results and on the right the theoretical results. The detail of the dicretization is also shown.

Figure 4a: The normalized stresses σ_{xx}/b_y for material Cu. The Burgers vector is **b**=(0, b_y). The isocontours range is (0.7, -0.7) Pa/m. On the left are the finite element results and on the right the theoretical results. The detail of the dicretization is also shown.

Figure 4b: The normalized stresses σ_{xx}/b_x for material Cu. The Burgers vector is **b**=(b_x, 0). The isocontours range is (0.7, -0.7) Pa/m. On the left are the finite element results and on the right the theoretical results. The detail of the dicretization is also shown.

Figure 5a: The normalized stresses σ_{xx}/b_y for material Cr. The Burgers vector is **b**=(0, b_y). The isocontours range is (2.0, -2.0) Pa/m. On the left are the finite element results and on the right the theoretical results. The detail of the dicretization is also shown.

Figure 5b: The normalized stresses σ_{xx}/b_x for material Cr. The Burgers vector is **b**=(b_x, 0). The isocontours range is (2.0, -2.0) Pa/m. On the left are the finite element results and on the right the theoretical results. The detail of the dicretization is also shown.

Figure 6: An edge dislocation at a distance *l* from the free surface.

Figure 7: The normalized stresses σ_{xx}/b_y for material W near the free surface. The Burgers vector is **b**=(0, b_y). The isocontours range is (1.0, -1.0) Pa/m. On the left are the finite element results and on the right the theoretical results. The detail of the dicretization is also shown.

Fig 1 A.E. Giann., K.P. Baxev., A. Gould

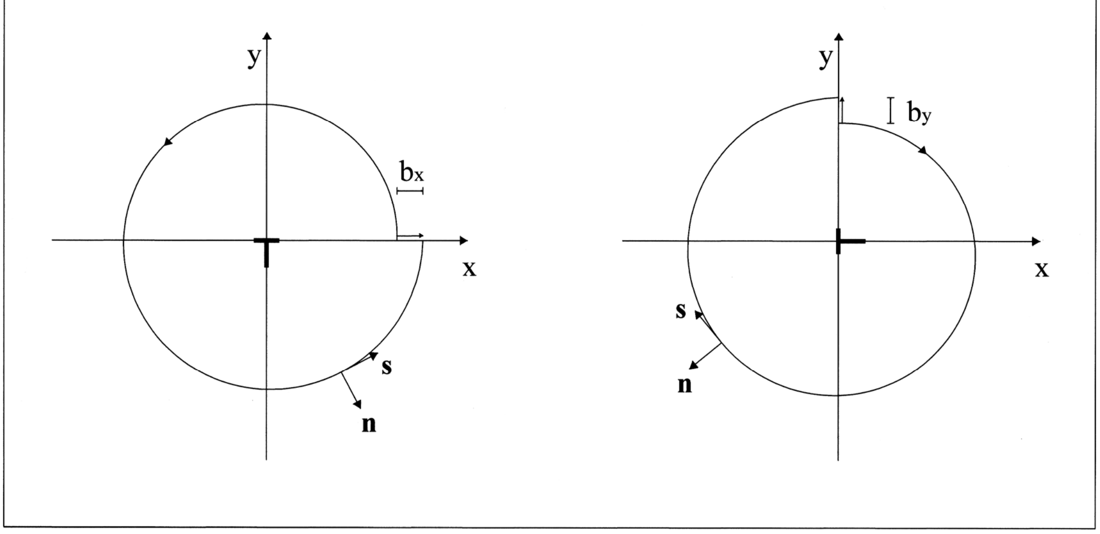

Fig 2 A.E. Giann., K.P. Baxev., A. Gould

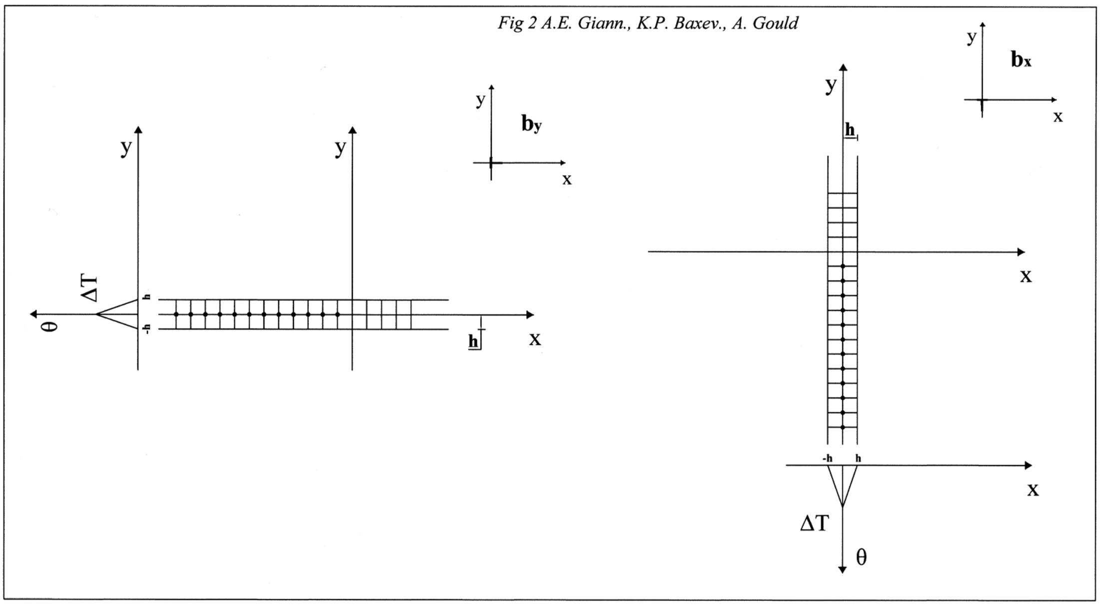

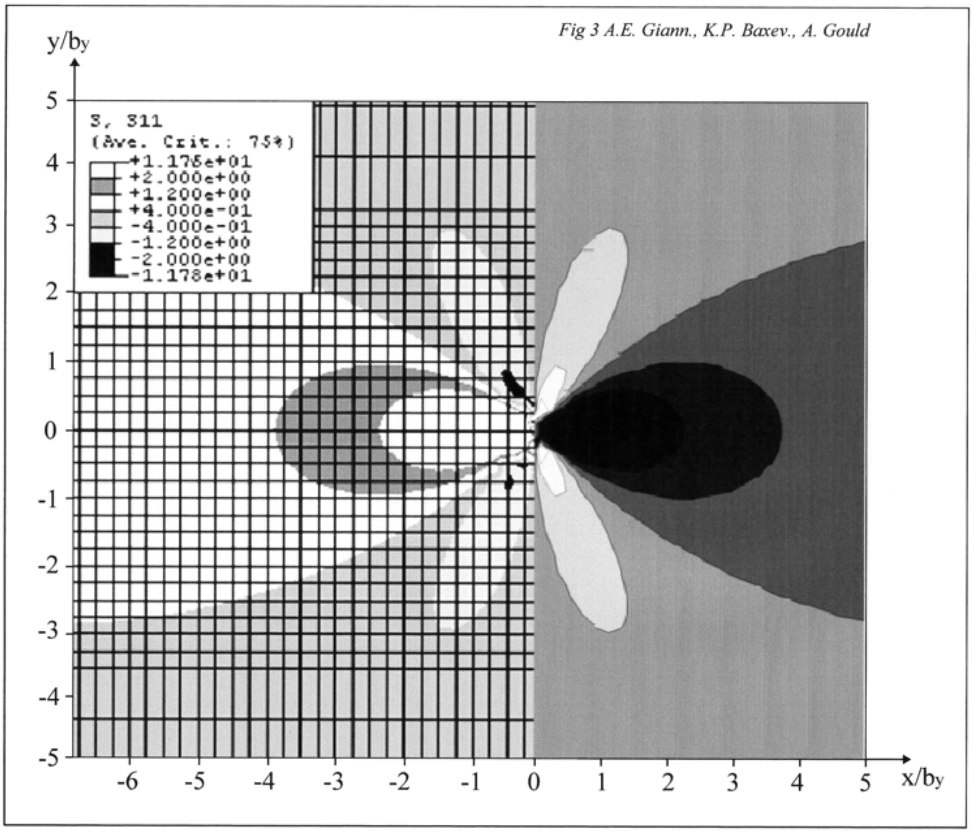
Fig 3 A.E. Giann., K.P. Baxev., A. Gould
y/by
x/by
S, S11
(Ave. Crit.: 75%)
+1.178e+01
+2.000e+00
+1.200e+00
+4.000e-01
-4.000e-01
-1.200e+00
-2.000e+00
-1.178e+01

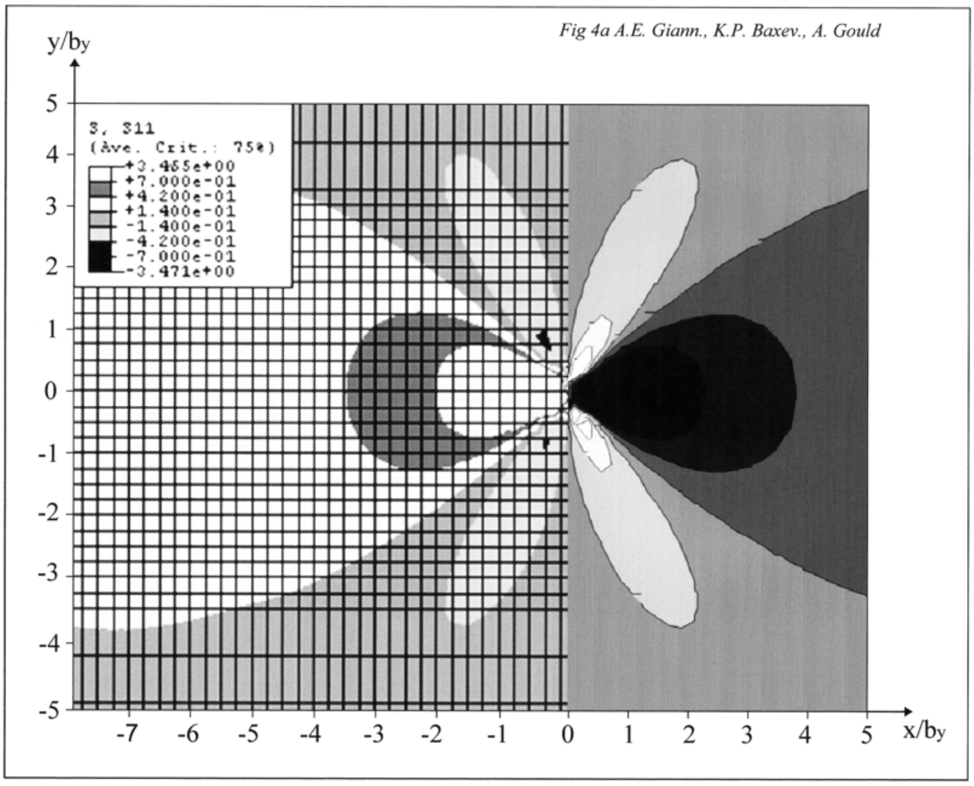
Fig 4a A.E. Giann., K.P. Baxev., A. Gould
y/by
x/by
S, S11
(Ave. Crit.: 75%)
+3.455e+00
+7.000e-01
+4.200e-01
+1.400e-01
-1.400e-01
-4.200e-01
-7.000e-01
-3.471e+00

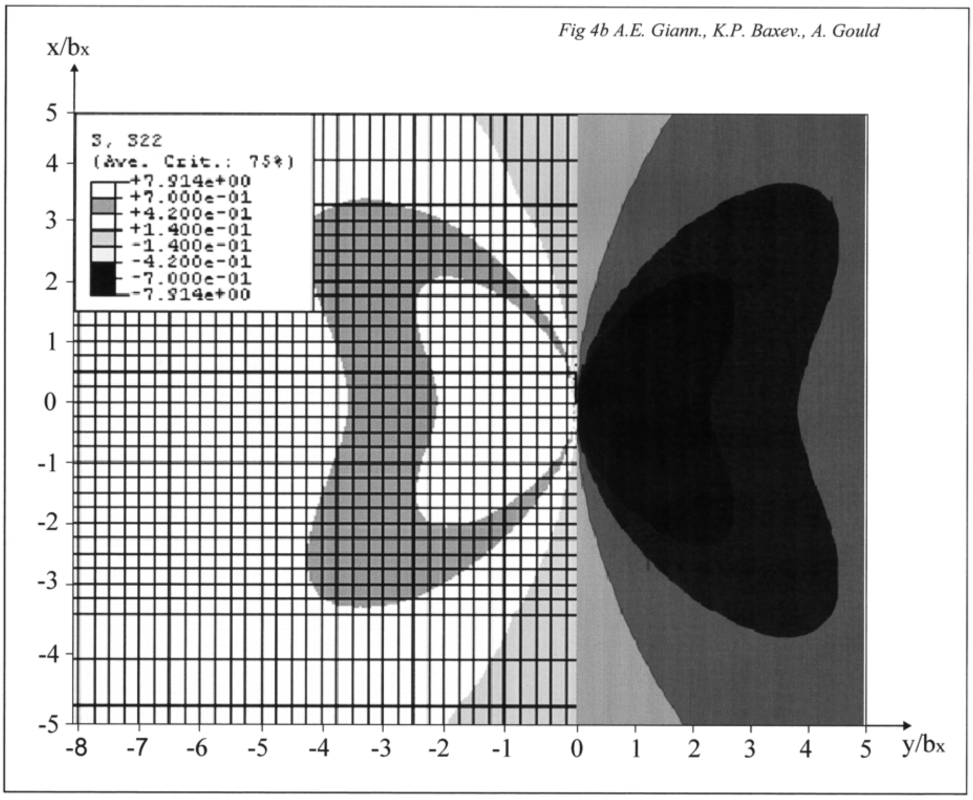
Fig 4b A.E. Giann., K.P. Baxev., A. Gould
x/bx
y/bx
S, S22
(Ave. Crit.: 75%)
+7.914e+00
+7.000e-01
+4.200e-01
+1.400e-01
-1.400e-01
-4.200e-01
-7.000e-01
-7.914e+00
5
4
3
2
1
0
-1
-2
-3
-4
-5
-8
-7
-6
-5
-4
-3
-2
-1
0
1
2
3
4
5

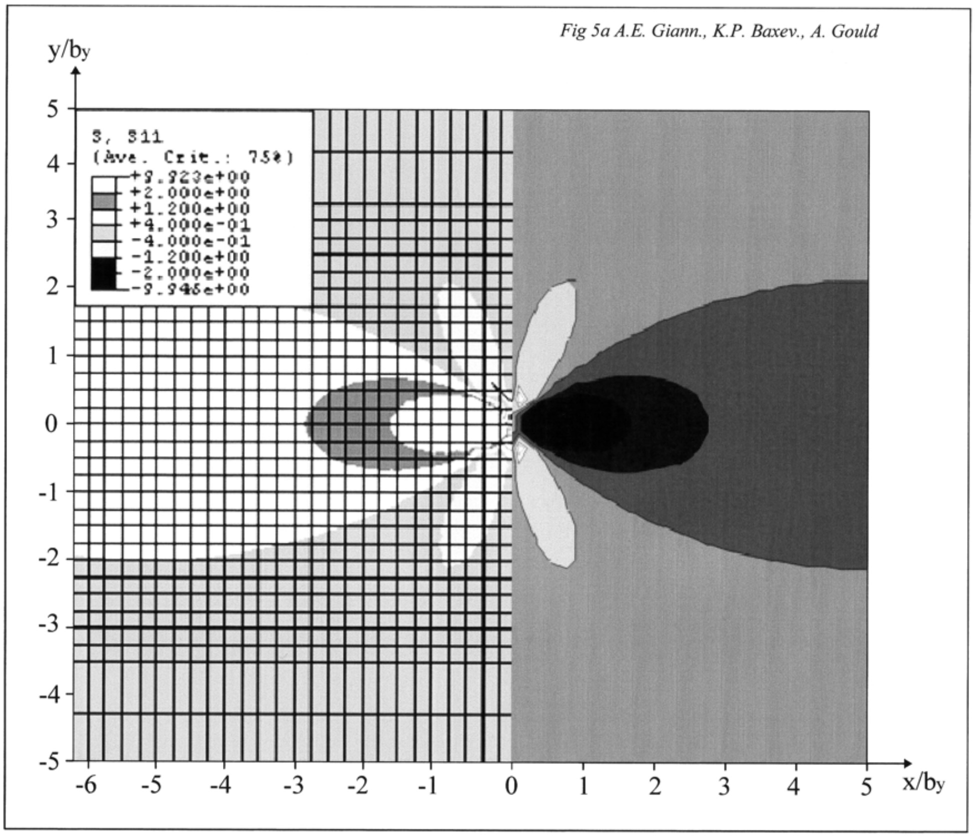
Fig 5a A.E. Giann., K.P. Baxev., A. Gould
y/by
x/by
S, S11
(Ave. Crit.: 75%)
+9.923e+00
+2.000e+00
+1.200e+00
+4.000e-01
-4.000e-01
-1.200e+00
-2.000e+00
-9.946e+00
5
4
3
2
1
0
-1
-2
-3
-4
-5
-6
-5
-4
-3
-2
-1
0
1
2
3
4
5

Fig 5b A.E. Giann., K.P. Baxev., A. Gould

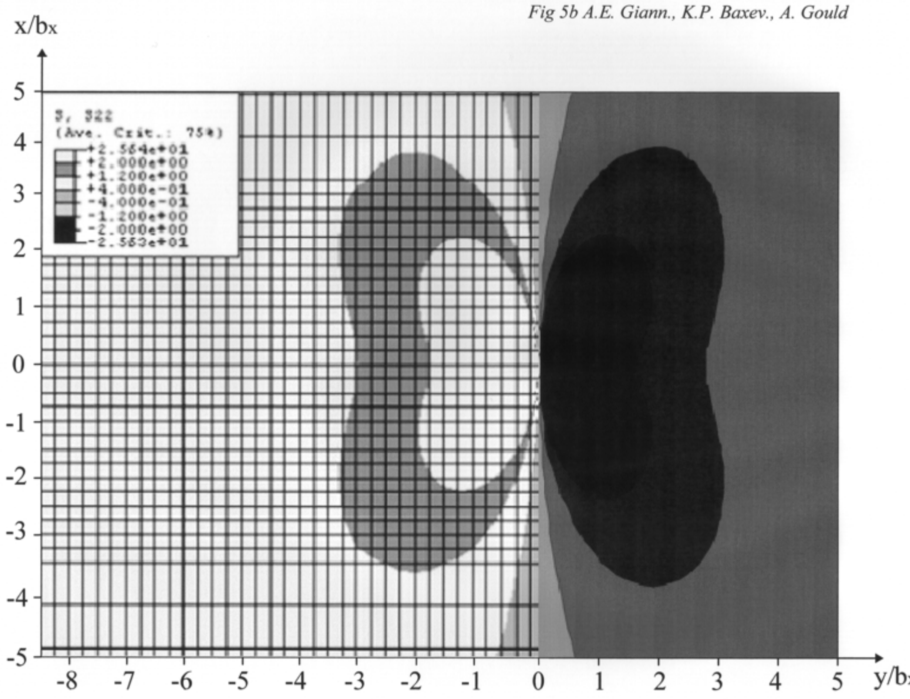

Fig 6 A.E. Giann., K.P. Baxev., A. Gould

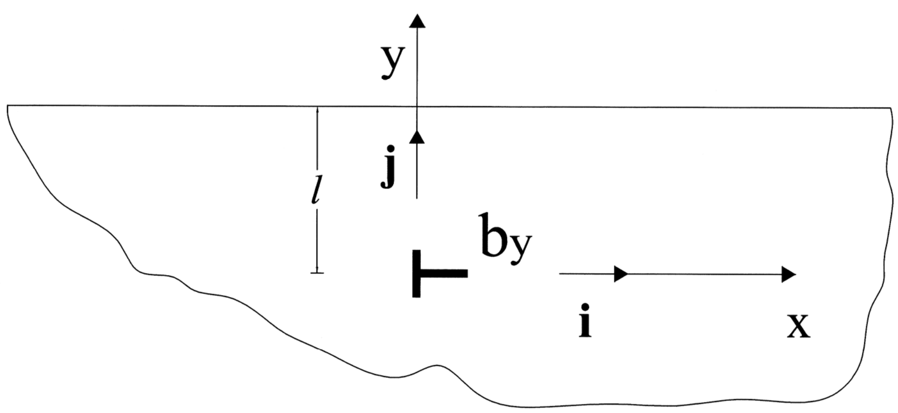

Fig 7 A.E. Giann., K.P. Baxev., A. Gould